Progress In Electromagnetics Research B, Vol. 52, 117–137, 2013

ANALYSIS OF THE CYCLOTRON RADIATION FROM RELATIVISTIC ELECTRONS INTERACTING WITH A RADIO-FREQUENCY ELECTROMAGNETIC WAVE

Christos Tsironis*

Department of Physics, Aristotle University of Thessaloniki, Thessaloniki 54 124, Greece

Abstract—The emission of electromagnetic radiation from charged particles spiraling around magnetic fields is an important effect in astrophysical and laboratory plasmas. In theoretical modeling, issues still not fully resolved are, among others, the inclusion of the recoil force on the relativistic electron motion and the detailed computation of the radiation power spectrum. In this paper, the cyclotron radiation emitted during the nonlinear interaction of relativistic electrons with a plane electromagnetic wave in a uniform magnetic field is examined, by analyzing the radiated power in both time and frequency domain. The dynamics of the instantaneous radiation and the emitted power spectrum from one particle, as well as from monoenergetic electron ensembles (towards a picture of the radiation properties independent of the initial conditions) is thoroughly studied. The analysis is performed for several values of the wave amplitude, focusing near the threshold for the onset of nonlinear chaos, in order to determine the alteration of the radiation in the transition from regular to chaotic motion.

1. INTRODUCTION

An important factor in systems involving charged particle acceleration by electromagnetic waves, especially for diagnostic measurements, is the emitted radiation by the particles due to the acceleration induced by the total acting electromagnetic force. Every charged particle, when accelerated, emits electromagnetic radiation (the relevant theory is analyzed sufficiently in [1–5]). The emitted radiation, apart from revealing the dynamics of the particle motion through its power spectrum, results to the appearance of an additional braking force on

Received 31 March 2013, Accepted 22 May 2013, Scheduled 26 May 2013

* Corresponding author: Christos Tsironis (ctsironis@astro.auth.gr).

the particle motion, known as radiation reaction [6]. With respect to the emission mechanism, the radiation is distinguished between two types: (a) Bremsstrahlung, coming from the component of the acceleration colinear with the particle velocity, and therefore relevant to the ballistic part of the motion, (b) Cyclotron, coming from the acceleration component perpendicular to the velocity, and therefore connected to the rotating part of the motion.

The cyclotron radiation from energetic electrons that rotate around a nearly static and homogeneous magnetic field is an aspect that appears frequently in astrophysical plasmas, like stellar winds ([7, 8] and references therein) or ionized atmospheric layers [9, 10]. The power spectrum of the radiation, as a measured quantity, gives valuable information for the plasma location, composition and dynamic behavior. In the laboratory, the accurate estimation of the electron-cyclotron radiation, beyond the conventional modeling based on black-body emission, is important for the assessment of the synchrotron radiation losses in accelerators [11] and thermonuclear devices [12, 13]. Regarding the latter, the gross of the radiated energy and the amount of its reabsorption by the ambient plasma [14] determine the global efficiency of the projected electrical power production.

The presence of an electromagnetic wave, as an additional force on the magnetized electrons, has been proved to enhance the acceleration when a resonance exists between the relativistic cyclotron motion and the Doppler-shifted wave frequency [15–17]. In the specific system, acceleration comes as a result of the overlapping of wave-particle resonances of different order in phase space, and therefore is of chaotic nature, contrary to the coherent acceleration achieved in inhomogeneous plasmas by adjusting the electron-cyclotron resonance layer [18]. Regarding the electron radiation, apart from the magnetic field also the circular polarization of the electromagnetic wave drives the electrons to fast rotating motions, therefore the emitted radiation is dominantly cyclotron. The frequencies of the emitted radiation are the same in which the electrons absorb electromagnetic waves due to the cyclotron resonance effect.

In this paper, the cyclotron radiation emitted during the nonlinear interaction of relativistic electrons with a uniform magnetic field and a plane electromagnetic wave is analyzed in both time and frequency domain. In time-domain, the study is the computation of the instantaneous power of emitted radiation, which is proportional to the acceleration and therefore its evolution is determined by the Lorentz force acting on the particle. In the frequency domain, one investigates the form of the radiation spectrum in comparison with the

motion in the absence of external forcing, for electrons in all velocity ranges. With respect to the above, an important issue is the self-consistent computation of the electron motion, taking into account the deceleration due to the radiation losses by including the higher-order radiation reaction term in the equations of motion. Here we do not deal with this issue, adopting the usual assumption that the amount of radiation emitted by each electron is reabsorbed by the other plasma electrons. The analysis is performed for many values of the wave amplitude, near and far from the threshold of nonlinear chaos, so that a clear picture is obtained for the alteration of the radiation towards the dynamic transition from order to chaos.

The structure of the paper is as follows: In Section 2 the Hamiltonian theory for the nonlinear interaction of relativistic electrons with a plane electromagnetic wave in a magnetic field is shortly reproduced, and in Section 3 the computation of the electron-cyclotron radiated power in time and frequency domain is presented. Then, in Section 4 the numerical results are shown, and finally in Section 5 the results are summarized, the limitations of our model are discussed and the issues prominent for future work are highlighted.

2. FORMULATION OF THE ELECTRON MOTION

The physics problem under study is the nonlinear interaction of relativistic electrons with a monochromatic plane electromagnetic wave, with frequency ω_0 and wave-number $\bar{k}$, propagating in the (x, z) plane at an angle ϑ with respect to a uniform magnetic field $\bar{B}_0 = B_0\hat{z}$ [17, 19]. The wave is considered as right-handed circularly polarized, whereas the background plasma is assumed to be cold. In this framework, the wave dispersion relation reads [18]

$$\tan^2\vartheta = -\frac{\mathcal{P}(N^2-\mathcal{C})(N^2-\mathcal{A})}{(N^2-\mathcal{P})(\mathcal{S}N^2-\mathcal{C}\mathcal{A})}. \tag{1}$$

In Eq. (1), $\bar{N} = c\bar{k}/\omega_0$ is the refraction index, which is decomposed to the Cartesian components $N_x = N\cos\vartheta$ and $N_z = N\sin\vartheta$ in the direction perpendicular and parallel to the magnetic field, and $\mathcal{P}$, $\mathcal{C}$, $\mathcal{A}$, $\mathcal{S}$ are the Stix parameters for cold plasma dispersion.

The combined effect of the wave and the plasma magnetic field on the electron is expressed via the vector potential $\bar{A}$ [19]

$$\bar{A} = A_0(\cos\vartheta\sin\varphi\hat{x} + \cos\varphi\hat{y} - \sin\vartheta\sin\varphi\hat{z}) + xB_0\hat{y}, \tag{2}$$

where $A_0 = E_0/\omega_0$ is the vector potential amplitude (E_0 the amplitude of the wave electric field), and φ is the wave phase, equal to

$$\varphi = \bar{k}\cdot\bar{r} - \omega_0 t = \omega_0\left[\frac{1}{c}(N_x x + N_z z) - t\right]. \tag{3}$$

The Lagrangian function for the relativistic electron motion, expressed in Cartesian coordinates ($\bar{r} = x\hat{x} + y\hat{y} + z\hat{z}$), is [20]

$$L = -m_e c^2 \left(1 - \frac{\dot{x}^2 + \dot{y}^2 + \dot{z}^2}{c^2}\right)^{1/2} - q_e(\dot{x}A_x + \dot{y}A_y + \dot{z}A_z). \quad (4)$$

Using Eq. (4), the calculation of the canonical momenta π_i (the canonical coordinates are $\xi_i = x, y, z$) is straightforward

$$\pi_i = \frac{\partial L}{\partial \dot{\xi}_i} = m_e \dot{\xi}_i \left(1 - \frac{\dot{x}^2 + \dot{y}^2 + \dot{z}^2}{c^2}\right)^{-1/2} - q_e A_i. \quad (5)$$

Putting Eqs. (4), (5) into the Liouville transformation relation of the Lagrangian function, $H = \bar{\pi} \cdot \dot{\bar{\xi}} - L$, yields the Hamiltonian function H of the system. By normalizing the Hamiltonian with $m_e c^2$ and the time t with ω_c^{-1}, and also using (2) to obtain the vector potential components, the following expression for H is derived

$$H = \left[1 + (\pi_x + A_0 \cos\vartheta \sin\varphi)^2 + (\pi_y + x + A_0 \cos\varphi)^2 + (\pi_z - A_0 \sin\vartheta \sin\varphi)^2\right]^{1/2}. \quad (6)$$

In (6), for the sake of simplicity, we use the same notations for the physical and the normalized quantities. Therefore, the normalized coordinates x, y and z are actually $c^{-1}\omega_c x$, $c^{-1}\omega_c y$ and $c^{-1}\omega_c z$, the normalized momenta π_x, π_y and π_z are similarly $(m_e c)^{-1}\pi_x$, $(m_e c)^{-1}\pi_y$ and $(m_e c)^{-1}\pi_z$ and the normalized vector potential amplitude A_0 is $m_e^{-1} q_e A_0$. In this context, normalizing also the wave frequency ω_0 with ω_c, the dimensionless phase φ is written as

$$\varphi = \omega_0 \left(N_x x + N_z z - t\right). \quad (7)$$

Notice here that, since the Hamiltonian does not depend explicitly on the coordinate y, the canonical momentum π_y is a constant of motion.

The Hamiltonian function of Eq. (6) is time-dependent because the wave phase, as one can easily detect from (7), is an explicit function of time. Non-autonomous dynamical systems are known to be rigorous in analyzing (see, e.g., [20]), and for that reason it is preferable to eliminate the presence of time by the means of a canonical transformation. The corresponding generating function is

$$\mathcal{F} = x'\pi_x + y'\pi_y + \left(z' - \frac{t}{N_z}\right)\pi_z, \quad (8)$$

where, for simplicity reasons, the old canonical variables and Hamiltonian are denoted as primed and the new ones as unprimed. The canonical variables and the Hamiltonian function may be found

from the transformation relations defined by the generating function

$$\begin{aligned}
\pi'_x &= \frac{\partial \mathcal{F}}{\partial x'} = \pi_x, \\
x &= \frac{\partial \mathcal{F}}{\partial \pi_x} = x', \\
\pi'_y &= \frac{\partial \mathcal{F}}{\partial y'} = \pi_y, \\
y &= \frac{\partial \mathcal{F}}{\partial \pi_y} = y', \\
\pi'_z &= \frac{\partial \mathcal{F}}{\partial z'} = \pi_z, \\
z &= \frac{\partial \mathcal{F}}{\partial \pi_z} = z' - \frac{t}{N_z}, \\
H &= H' + \frac{\partial \mathcal{F}}{\partial t} = \gamma - \frac{\pi_z}{N_z}.
\end{aligned} \tag{9}$$

In the above relations, γ is the relativistic Lorentz factor (and also the normalized energy of the electron), given by $\gamma = H'$, with H' as given in (6), and φ the new (time-independent) wave phase as given in (7) with the omission of the term $-t$.

The above formulation provides us with the equations of the electron motion, which determine the dynamics of the system. The exact equations can be easily derived from the Hamiltonian function, and are written in normalized form as follows

$$\begin{aligned}
\frac{dx}{dt} &= \frac{\partial H}{\partial \pi_x} = \frac{\pi_x}{\gamma} + \frac{A_0 \cos\vartheta \sin\varphi}{\gamma}, \\
\frac{dy}{dt} &= \frac{\partial H}{\partial \pi_y} = \frac{\pi_y}{\gamma} + \frac{x}{\gamma} + \frac{A_0 \cos\varphi}{\gamma}, \\
\frac{dz}{dt} &= \frac{\partial H}{\partial \pi_z} = \frac{\pi_z}{\gamma} - \frac{A_0 \sin\vartheta \sin\varphi}{\gamma} - \frac{1}{N_z}, \\
\frac{d\pi_x}{dt} &= -\frac{\partial H}{\partial x} = \omega_0 A_0 N_x \frac{\mu}{\gamma} - \frac{\pi_y}{\gamma} - \frac{x}{\gamma} - \frac{A_0 \cos\varphi}{\gamma}, \\
\frac{d\pi_y}{dt} &= -\frac{\partial H}{\partial y} = 0, \\
\frac{d\pi_z}{dt} &= -\frac{\partial H}{\partial z} = \omega_0 A_0 N_z \frac{\mu}{\gamma},
\end{aligned} \tag{10}$$

in which the kinematic quantity μ is equal to $\mu = (\pi_y + x)\sin\varphi + \pi_z \sin\vartheta \cos\varphi - \pi_x \cos\vartheta \cos\varphi$.

Some of the aspects of the electron dynamics that are stimulating for the form of the cyclotron radiation are highlighted, on the basis of the numerical solution of Eq. (10). The system parameters are relevant to wave heating experiments of the night-time ionosphere at an altitude 130 km: The magnetic field is $B_0 = 3.5 \cdot 10^{-5}\,\mathrm{T}$, giving a cyclotron frequency $\omega_c = 1.96\pi\,\mathrm{MHz}$, and the plasma density is $n_e = 10^2\,\mathrm{cm}^{-3}$, so the plasma frequency is $\omega_p = 0.564\,\mathrm{MHz}$. The wave frequency is $\omega_0 = 6\pi\,\mathrm{MHz}$, and the propagation angle is $\vartheta = 40^\circ$. Many values of the wave amplitude were used, for a normalized value A_0 corresponds to total power flux $S = 30\omega_0^2 A_0^2$ (Wcm^{-2}). The equations of motion are integrated using a 4th-order Runge-Kutta scheme with constant step $\Delta T = 0.01$, the accuracy of which was checked by the calculation error of the constant $H = 1.5$ (found to be of the order 10^{-9}).

In this system, chaotic motions appear if A_0 is larger than a critical value A_{0c} which depends on the other parameters (wave frequency and propagation angle). A local estimate of A_{0c} is found from the fact that only for $A_0 > A_{0c}$ is acceleration possible, as seen in Fig. 1(a) where the mean energy of an ensemble of 10000 electrons with initial energy $\gamma_0 = 2.5$ (1.279 MeV) at $t = 3000$ (0.48 ms) is plotted as a function of A_0. The energy remains almost constant for small A_0, until a sudden increase appears near $A_{0c} = 0.02$ (a value $S_c = 0.197\,\mathrm{Wcm}^{-2}$ for the power flux). The onset of chaos is similar with respect to the angle of propagation: For fixed values of the other parameters, there is a critical angle value over which chaos appears [17].

The interaction of electrons with a single wave is a system of two degrees of freedom, so the dynamics can be visualized using Poincarè surfaces of section. The intrinsic complexity of the phase space is pictured in Fig. 1(b), where the surface of section (x, π_x) is shown for $A_0 = 0.1$. This picture is built by following 50 electron orbits until $t = 3000$, and the section points are taken stroboscopically every time $\omega_0 N_z z$ is a multiple of 2π with the same direction of crossing ($\dot{z} < 0$). The appearance of islands in the surface of section, which correspond to phase-space trajectories of quasiperiodic orbits, occurs due to the matching of the wave phase with the electron rotation at certain regions of the phase space (for more details refer to [15, 17]). Electrons that move in the vicinity of such regions are not accelerated significantly by the wave, and could be characterized as "trapped" with respect to the energetic electron population appearing in the chaotic regions.

The distribution of the particle energies is important since the probability density function can be found as the solution of the Fokker-Planck equation [17], depending on the dynamical characteristics of the motion. In Fig. 1(c), the energy distribution function of an ensemble of 10000 particles with initial energy $\gamma_0 = 2.5$ is given for $A_0 = 0.1$

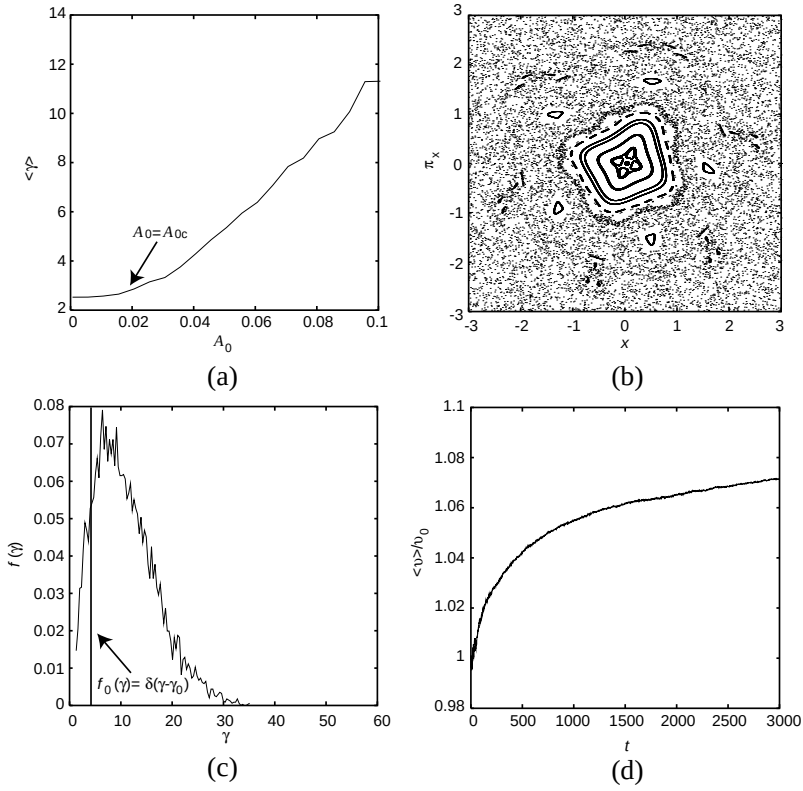

Figure 1. Visualizing the system dynamics for the parameters set above. (a) Mean energy vs wave amplitude. (b) Poincarè surface of section. (c) Energy distribution function. (d) Mean velocity vs time.

after $t = 5000$. The evolution of the system is clearly associated with energy gain from the acceleration of the electrons. This behavior is also seen in Fig. 1(d), where the normalized mean particle velocity is shown as a function of time for the same parameters.

3. THEORY OF CYCLOTRON RADIATION

An electron that rotates around the dynamic lines of a magnetic field emits electromagnetic radiation at the frequency of its rotation, hence referred to as cyclotron radiation [2], which emanates from the centripetal acceleration induced by the Lorentz force. The power of the cyclotron radiation emitted by the electron at a certain time instant is given by the Lienard formula [1, 2], which gives a valid description for

both classical and relativistic electron velocities

$$P_R = \frac{q_e^2}{6\pi\varepsilon_0 c^3}\gamma^6 \left[c^2 a^2 - |\bar{v}\times\bar{a}|^2\right]. \tag{11}$$

In the Lienard formula, P_R stands for the radiated power and $\bar{v}$, $\bar{a} = d\bar{v}/dt$ the velocity and acceleration vectors at the specific time instant. By normalizing P_R with $c^{-1}\varepsilon_0 q_e^2\omega_c$, $\bar{v}$ with c and $\bar{a}$ with $c\omega_c$, with the remaining quantities normalized in the same manner as in the previous section, one obtains the dimensionless version of Eq. (11). In the Cartesian coordinate system, this reads

$$P_R = \frac{\gamma^6}{6}\Big[a_x^2 + a_y^2 + a_z^2 - (v_y a_z - v_z a_y)^2 - (v_z a_x - v_x a_z)^2 - (v_x a_y - v_y a_x)^2\Big]. \tag{12}$$

Regarding the computation of P_R using Eq. (12), there is a point that should be noticed concerning the calculation of the velocity in terms of the conjugate variables: The canonical transformation (8), which was applied for the elimination of time from the Hamiltonian function, is not compatible with the Lorentz transformation structure. As a consequence, v_x, v_y, v_z should be calculated using the untransformed coordinate values. The latter issue does not prevent the expression of the velocities via the transformed coordinates, however this should be formulated consistently. In this spirit, by differentiating Eq. (9) over time one obtains the (normalized) velocity components in terms of x, y, z as follows

$$\begin{aligned} v_x &= \dot{x}, \\ v_y &= \dot{y}, \\ v_z &= \dot{z} + \frac{1}{N_z}. \end{aligned} \tag{13}$$

The normalized acceleration components a_x, a_y, a_z are found by taking the derivative over time of the physics relation $\bar{p} = m_e\gamma\bar{v}$, which delivers the relativistic mechanical momentum vector, and normalizing the momenta again by $m_e c$

$$\frac{d\bar{p}}{dt} = \frac{d(\gamma\bar{v})}{dt} = \gamma\bar{a} + \gamma^3(\bar{v}\cdot\bar{a})\bar{v}. \tag{14}$$

The Cartesian components of the time-derivative of the relativistic momentum can be written in terms of the canonical coordinates and their derivatives, following a differentiation of Eq. (5) over time and using also (2) for the vector potential components and the relevant relation for the wave phase

$$\begin{aligned} \dot{p}_x &= \dot{\pi}_x + \omega_0 A_0 \left(N_x\dot{x} + N_z\dot{z}\right)\cos\vartheta\cos\left[\omega_0\left(N_x x + N_z z\right)\right], \\ \dot{p}_y &= \dot{\pi}_y + \dot{x} - \omega_0 A_0 \left(N_x\dot{x} + N_z\dot{z}\right)\sin\left[\omega_0\left(N_x x + N_z z\right)\right], \\ \dot{p}_z &= \dot{\pi}_z - \omega_0 A_0 \left(N_x\dot{x} + N_z\dot{z}\right)\sin\vartheta\cos\left[\omega_0\left(N_x x + N_z z\right)\right]. \end{aligned} \tag{15}$$

Having computed $\dot{\bar{p}}$, the analysis of the vector Eq. (14) to Cartesian components provides us with three relations which, if reordered with respect to a_x, a_y, a_z, take the form of a linear set of algebraic equations with unknown quantities the acceleration components. The solution of this set is straightforward

$$\begin{aligned} a_x &= \frac{(1+\gamma^2 v_y^2+\gamma^2 v_z^2)\dot{p}_x - \gamma^2 v_x v_y \dot{p}_y - \gamma^2 v_x v_z \dot{p}_z}{\gamma(1+\gamma^2 v^2)}, \\ a_y &= \frac{-\gamma^2 v_x v_y \dot{p}_x + (1+\gamma^2 v_x^2+\gamma^2 v_z^2)\dot{p}_y - \gamma^2 v_y v_z \dot{p}_z}{\gamma(1+\gamma^2 v^2)}, \\ a_z &= \frac{-\gamma^2 v_x v_z \dot{p}_x - \gamma^2 v_y v_z \dot{p}_y + (1+\gamma^2 v_x^2+\gamma^2 v_y^2)\dot{p}_z}{\gamma(1+\gamma^2 v^2)}. \end{aligned} \tag{16}$$

Based on Eqs. (12), (13), and (16) including (15), together with the solution of the equations of motion coming from Eq. (10), the computation of the radiated power in time domain is achieved.

The frequency spectrum of the emitted radiation constitutes a powerful diagnostic for the identification of the plasma region under observation, providing, among others, the spatial extent, the ionization degree and the energetics of the system [1]. The obvious way to compute the radiated power in frequency domain is to apply a Fourier transform directly on the Lienard formula. However, since what is measured in practice is the radiated energy in a defined frequency band $\Delta\omega$ over a specific solid angle $\Delta\Omega$ around the observation point, the calculation is formally performed by finding the emitted energy per unit solid angle per unit frequency and integrating over all angles.

The emitted power per unit solid angle is a quantity that depends on the location of the observation point. For an electron radiating due to cyclotron motion and being observed from a distant point with respect to its trajectory spiral, the observation unit vector can be considered as independent of the orbit details, and therefore constant in time. In this framework, the emitted power per unit solid angle by a single electron, at past and future time instants, is given by [1, 2]

$$\frac{dP_R^F}{d\Omega} = \frac{q_e^2\omega^2}{16\pi^3\varepsilon_0 c}\left|\int_{-\infty}^{+\infty} \hat{r}' \times \hat{r}' \times \frac{\bar{v}}{c}\exp\left[i\omega\left(t - \frac{\hat{r}'\cdot\bar{r}}{c}\right)\right]dt\right|^2, \tag{17}$$

where P_R^F is the power of the cyclotron radiation in frequency domain, actually the Fourier transform of P_R, ω is the radiation frequency and $\hat{r}'$ is the unit vector in the direction of the observation point

$$\hat{r}' = \sin\theta\cos\phi\hat{x} + \sin\theta\sin\phi\hat{y} + \cos\theta\hat{z}, \tag{18}$$

with θ, ϕ the latitude and azimuth observation angle (see Fig. 2).

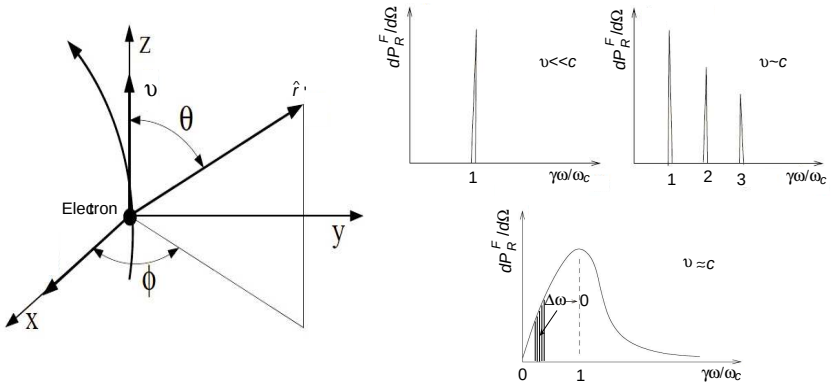

(a) (b)

Figure 2. Pictures from the theory of cyclotron radiation. (a) Proper coordinate system for the computation of the power spectrum. (b) Transition of the form of the spectrum from discrete to continuous (synchrotron) with the velocity increase.

Starting from Eq. (17), normalization of the solid angle Ω with 4π and of all the other quantities similarly to the previous derivations leads to a dimensionless relation for the radiated power

$$\frac{dP_R^F}{d\Omega} = \frac{\omega^2}{4\pi^2}\left|\int_{-\infty}^{+\infty} \hat{r}' \times \hat{r}' \times \bar{v} \exp\left[i\omega\left(t - \hat{r}' \cdot \bar{r}\right)\right] dt\right|^2. \qquad (19)$$

In Eq. (19), the exponent $t - \hat{r}' \cdot \bar{r}$ represents the principle of determinism in the fact that the radiation requires an amount of time to cover the distance between the electron and the observer, since it propagates with a finite velocity (at maximum equal to c). The complex integral of (19), symbolized with $\bar{\mathcal{I}}$ from this point on, is actually the factor forming the details of the frequency spectrum of the emitted radiation. $\bar{\mathcal{I}}$ is a vector that has real and imaginary parts, which are given by

$$\Re(\bar{\mathcal{I}}) + i\Im(\bar{\mathcal{I}}) = \int_{-\infty}^{+\infty} \left(\mathcal{V}\hat{r}' - \bar{v}\right) \exp\left[\omega\left(t - \mathcal{R}\right)\right] dt. \qquad (20)$$

In the process of obtaining Eq. (20) from (19), the vector identity $\hat{r}' \times \hat{r}' \times \bar{v} = (\hat{r}' \cdot \bar{v})\hat{r}' - \bar{v}$ was used, and the projections of the electron position and velocity vectors onto the direction of observation were introduced as $\mathcal{R} = \hat{r}' \cdot \bar{r}$ and $\mathcal{V} = d\mathcal{R}/dt = \hat{r}' \cdot \bar{v}$. The parameters $\mathcal{R}$, $\mathcal{V}$ are expressed in the Cartesian system as

$$\begin{aligned} \mathcal{R} &= x\sin\theta\cos\phi + y\sin\theta\sin\phi + z\cos\theta, \\ \mathcal{V} &= v_x\sin\theta\cos\phi + v_y\sin\theta\sin\phi + v_z\cos\theta. \end{aligned} \qquad (21)$$

Inserting Eqs. (18) and (21) into Eq. (20) leads to a form of the six components of $\bar{\mathcal{I}}$ that depends only on kinematic variables. This implies that the numerical computation of $\bar{\mathcal{I}}$ may be performed with Riemann summation of the involved quantities along the electron orbits. A much faster method to evaluate the integrals is by using a fast (discrete) Fourier transform [21], which is partially allowed by the form of the integrated function. In order to conform with the method, the exponent must be strictly of the form ωt, so the part $-\omega\mathcal{R}$ must vanish. This is achieved by a change in the integration variable t according to the transformation

$$\begin{aligned} t' &= t - \mathcal{R}, \\ dt' &= (1 - \mathcal{V})dt. \end{aligned} \tag{22}$$

The choice of the symbol t' for the new integration variable has been based on its physics meaning as the system time measured by the observer. In terms of t', the integral $\bar{\mathcal{I}}$ takes the Fourier form and its numerical evaluation is easy. The real part of the integral is

$$\begin{aligned} \Re(\mathcal{I}_x) &= \int_{-\infty}^{+\infty} \left.\frac{\mathcal{V}\sin\theta\cos\phi - v_x}{1-\mathcal{V}}\right|_{t=t'+\mathcal{R}} \cos\omega t' dt', \\ \Re(\mathcal{I}_y) &= \int_{-\infty}^{+\infty} \left.\frac{\mathcal{V}\sin\theta\sin\phi - v_y}{1-\mathcal{V}}\right|_{t=t'+\mathcal{R}} \cos\omega t' dt', \\ \Re(\mathcal{I}_z) &= \int_{-\infty}^{+\infty} \left.\frac{\mathcal{V}\cos\theta - v_z}{1-\mathcal{V}}\right|_{t=t'+\mathcal{R}} \cos\omega t' dt', \end{aligned} \tag{23}$$

and for the imaginary part what changes is the term $\sin\omega t'$ instead of $\cos\omega t'$. In Eq. (23), the values of the integrand are calculated at the time instant t that corresponds, through (22), to the desired t' value.

For the motion of a magnetized electron in the presence of an electromagnetic wave, the spectrum of the emitted radiation has a lot of similarities with the spectrum of the pure cyclotron motion, since the rotational part is more energetic than the motion along the magnetic field. The dependence of the spectrum on the electron energy is visualized in Fig. 2(b). For small electron energy ($\beta = v/c \ll 1$), the electric field of the radiation oscillates with frequency equal to the cyclotron frequency, therefore the spectrum consists of only one line at $\omega = \omega_c$. As v increases, contributions from the higher harmonics start to appear, and for velocities near c the lines are so close that the spectrum is practically continuous. This behavior is owed to the fact that, within the relativistic theory, a rotating electron emits radiation at all frequency harmonics $n\omega_c/\gamma$ with amplitude proportional to β^n [1]. This means that as the electron velocity increases, the spectral lines at higher frequency appear more enhanced.

Another typical characteristic of the emission received at an observation point is the Doppler shift of the spectral lines [1, 2]. This happens because the period of oscillations in the wave frame is different than the one in the observer frame due to the relativistic time dilation. This frequency shift is demonstrated if Eq. (20) is expressed in terms of the Fourier transform of the integrand function

$$\bar{\mathcal{I}} = \int_{-\infty}^{\infty} \left\{ \mathrm{FT}\left(\mathcal{V}\hat{r}' - \bar{v}\right) \int_{-\infty}^{\infty} \exp\left[it\left(\omega - \omega\dot{\mathcal{R}} - \omega'\right)\right] dt \right\} d\omega', \quad (24)$$

which, by using the exponential representation of the δ-function, yields

$$\bar{\mathcal{I}} = \int_{-\infty}^{\infty} \mathrm{FT}\left(\mathcal{V}\hat{r}' - \bar{v}\right) \delta\left[\omega' - \omega\left(1 - \mathcal{V}\right)\right] d\omega'. \quad (25)$$

(25) implies that the position of the spectral lines is determined by the delta function inside the integral, which allows for nonzero values of $\bar{\mathcal{I}}$ only for frequencies $\omega^* = \omega(1 - \mathcal{V})$. The latter verifies that the spectrum lines are upshifted from the expected ones by a factor $\omega\mathcal{V}$.

In applying the above formulation as a numerical computation scheme, one should consider few practical issues. First, the infinite-limit integrals emanating from $\bar{\mathcal{I}}$ are calculated over a finite-time interval starting from $t = 0$, however this is typically handled by the fast Fourier transform algorithm. Second, the change of the integration variable (22), when computing the power density in (19) from a time sample, creates an unequally-spaced t'-sample, since it is $\Delta t' \approx (1 - \mathcal{V})\Delta t$. This inconsistency is resolved with the creation of a new, equally-spaced sample by laying a grid of equally-spaced values of t' and interpolate the integrand values onto that grid before the use of the discrete Fourier transform method.

4. NUMERICAL RESULTS

In this section, numerical results from the computation of the cyclotron radiation by magnetized electrons interacting with an (external) electromagnetic wave are shown. The numerical scheme used, which has been presented in the previous sections, consists of the orbit data computation from the Hamiltonian model in Eq. (10), and, based on this data, the calculation of the instantaneous radiation power from Eq. (12) and the determination of the power spectrum from (19). The study begins by analyzing the time evolution of the instantaneous power from one particle, followed by a more general view, independent of the initial conditions. in terms of the mean power over a monoenergetic electron ensemble. Afterwards, the study moves to the frequency domain by considering the power spectrum of the radiation

emitted during the electron motion at different observation directions. The above are repeated for many values of the wave amplitude, over and under the threshold to chaos, in order to examine the radiation behavior during the transition from ordered to chaotic motion.

The electron orbit data has been computed for the values of ω_0, B_0, n_e, ϑ and H already mentioned in Section 2. The amplitude A_0, dynamically viewed as a perturbation strength, has been assigned in the range [0, 0.5]. The canonical equations were integrated for electrons of the same initial energy γ_0 (or velocity β_0) and the following initial conditions: x_0 chosen randomly within the energetic-permissible region of the (x, π_x) phase subspace, using a Parks-Miller random number generator [21], y_0, z_0 set equal to zero, π_{x0} found from (6) for the corresponding values of A_0 and x_0, the constant of motion π_{y0} set 0.03 and π_{z0} calculated from (9). It should be stated that the quantities by which we normalize the electron kinetic energy and the radiated energy are very different, with the first being of order $\sim 10^{20}$ greater (this should be considered in case comparisons are attempted).

The time signal of the radiation from a single particle, as calculated from the Lienard formula using numerical values for the velocity and acceleration, is shown in Fig. 3 for different values of the wave amplitude. For $A_0 < A_{0c}$ (see Section 2 for the definition of A_{0c}), the problem is much close to a cyclotron motion around the magnetic lines, in which case P_R is nearly constant over time. This is reproduced in Fig. 3(a), where P_R vs t is plotted for $A_0 = 0.02$. A quick description can be given in terms of the Lienard formula, which is simplified to

$$P_R = \frac{\gamma^6 a^2}{6} \left(1 - v^2 \sin^2 \chi\right), \tag{26}$$

with χ the angle between $\bar{v}$ and $\bar{a}$. The power oscillates throughout the orbit, depending on the velocity, acceleration and the orbit curvature, quantities all constant in cyclotron motion. For $A_0 > A_{0c}$, P_R begins to vary slightly because the electron motion starts to diverge from simple gyration as the threshold to chaos is crossed, and this is seen in Fig. 3(b). In Section 2 it was shown that, for the specific values of the system parameters, the perturbation threshold for the initiation of stochastic acceleration is $A_{0c} \sim 0.02$. Therefore, and since $P_R \propto a^2$, the radiated power follows a behavior similar to that of the acceleration.

As A_0 increases, the radiated power fluctuates more intensively, remaining though confined in a range that gradually expands with A_0. It is obvious that the larger A_0 becomes, the larger should be the power during the orbit. This is shown in Fig. 3(c), where P_R is plotted vs t for $A_0 = 0.1$. After sufficient time (over 1500), the radiation starts to increase irregularly and presents variations larger than before, and this behavior intensifies for larger A_0. The explanation lies in the fact that

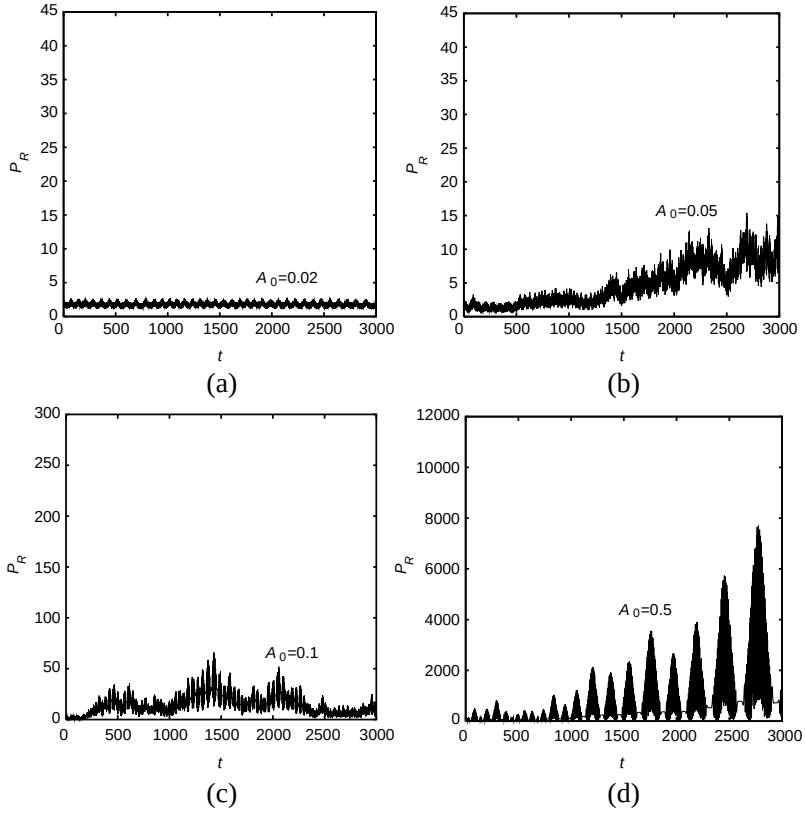

Figure 3. Time signal of the instantaneous power emission by one electron for four different values of the wave amplitude. (a) $A_0 = 0.02$. (b) $A_0 = 0.05$. (c) $A_0 = 0.1$. (d) $A_0 = 0.5$.

for $A_0 \gg A_{0c}$ the wave-electron interaction becomes much stronger, resulting to a significant augmentation in electron acceleration. In addition, the fluctuations of the power tend to occur at an increasingly organized fashion, becoming isolated at distinguishable time intervals. For large amplitude, like $A_0 = 0.5$ in Fig. 3(d), one could actually say that the main volume of radiation is emitted at certain time fractions, with small pauses during which the radiation power remains constant at a relatively small value. In an effort to connect all these facts with the electron orbit, one could say that the power of each pulse is characteristic of the wave-electron interaction intensity.

The above provide the main aspects of the emitted power from a single electron in time domain. The choice of initial conditions may give rise to different results, but should not affect the qualitative

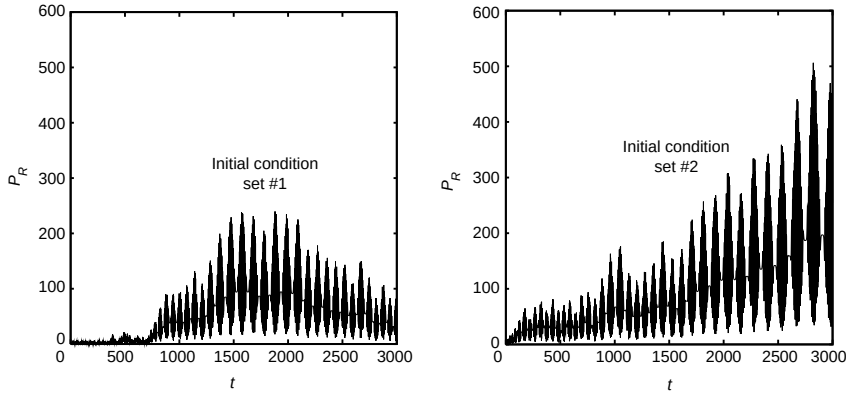

Figure 4. Time signal of the instantaneous power emission by one electron for $A_0 = 0.2$ and two different sets of initial conditions.

properties. This is verified in Fig. 4, where a comparison is made between two initial condition sets, randomly different in π_{x0}, for $A_0 = 0.2$. The form of the two signals is very similar, apart from the periodicity of the power variation and the total emission. Such differences emanate from the inhomogeneity of the phase space with respect to the electron dynamics, which distinguish the orbits in trapped and unbounded depending on the initial conditions. Consequently, for making more general considerations on the emitted radiation, independent of the particle orbit details, the transition to an average of the above results over the phase space is obligatory.

In this spirit, the mean value of the instantaneous power over an ensemble of 1000 electrons with $\gamma_0 = 2.5$ is evaluated. The use of $\langle P_R \rangle$ annihilates the differences arising from the inhomogeneity of the phase space, for it is the average over many electrons with random initial conditions. In Fig. 5 we show the result for three different values of A_0, near and over the threshold A_{0c}. Similarly to the considerations made above for one particle, for small values of A_0 the power starts fluctuating around its constant value, and as A_0 overcomes A_{0c} chaotic motions start to form a majority in phase space and P_R increases with time. This becomes more evident from Fig. 5(b) for $A_0 = 0.5$. The fluctuations in the results owe their presence to the finite number of test particles used (a larger ensemble would yield a more confined curve).

Going now to the frequency domain, the form of the angular power spectrum of the cyclotron radiation from a magnetized electron interacting with a radio-frequency wave is given in Fig. 6, in two

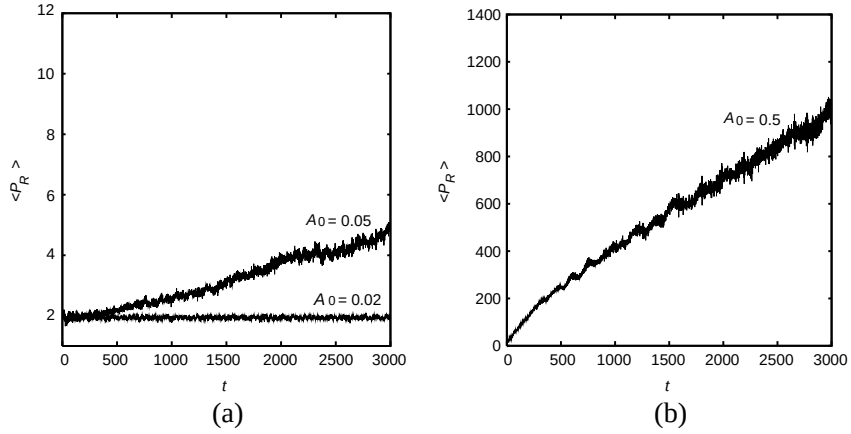

Figure 5. Average power emission vs time of 1000 electrons with the same initial energy for three different values of the wave amplitude.

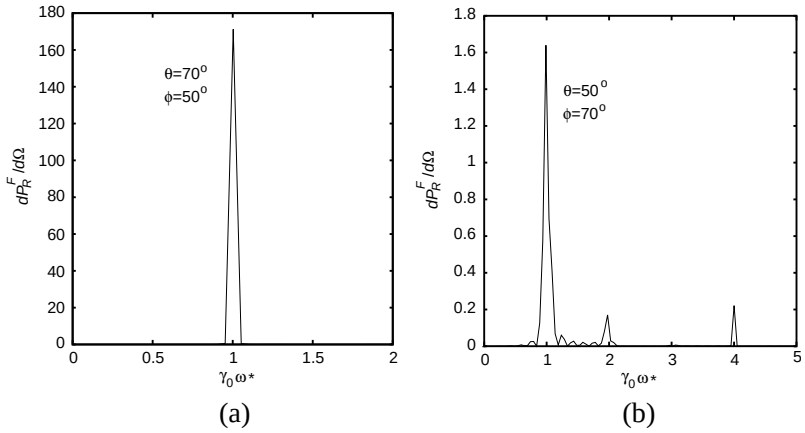

Figure 6. Angular power spectrum of the cyclotron radiation from an electron of initial velocity $\beta_0 = 0.4$ interacting with a radio-frequency wave of amplitude $A_0 = 0.05$, at two different observation directions (a) $\theta = 70°$, $\phi = 50°$ and (b) $\theta = 50°$, $\phi = 70°$.

different observation directions: (a) $\theta = 70°$, $\phi = 50°$, and (b) $\theta = 50°$, $\phi = 70°$. For the specific computation, the wave amplitude is $A_0 = 0.05$, the electron initial velocity is $\beta_0 = 0.4$ and the rest of the parameters and initial conditions are specified in the way mentioned already in the beginning of this section. Notice that, for convenience,

the spectrum is expressed in terms of the canonical frequencies ω^* instead of the Doppler-shifted ones. In both cases, the spectrum appears similar to the typical picture of the cyclotron radiation for this velocity. However, a comparison of the two cases shows that the spectra are much different: In the first direction only the fundamental mode is observed, whereas along the second one significant contributions from higher harmonics are seen. This effect implies that the angular power spectrum has a sensitive dependence on the observation direction.

In this sense, to use the angular power spectrum for the accurate estimation of the electron emission is not completely justified and may be misleading. One should then resort to the standard implementation of the power spectrum, which, in the frequency domain, is to express the emitted energy per unit frequency as a function of the frequency. From this scope, the power spectrum may be computed by integrating numerically the angular power density over all directions of observation

$$P_R^F = \int_0^{2\pi} \int_0^{\pi} \frac{dP_R^F}{d\Omega} \sin\theta d\theta d\phi. \tag{27}$$

The power spectrum of the cyclotron radiation, integrated over all angles, is visualized in Fig. 7 for four combinations of A_0, β_0: (a) $A_0 = 0.1$, $\beta_0 = 0.05$, (b) $A_0 = 0.02$, $\beta_0 = 0.4$, (c) $A_0 = 0.1$, $\beta_0 = 0.4$, and (d) $A_0 = 0.1$, $\beta_0 = 0.9$. As in the previous figure, in all cases the spectrum has a lot of similarities with the radiation pattern shown in Fig. 2. In case (a), where the electron is non-relativistic, the spectrum is discrete and contains only the fundamental harmonic, whereas in case (c), for the same A_0 and the electron being mildly-relativistic, except from the fundamental there is measurable excitation also from many of the higher harmonics. Notice that the spectral lines do not appear at the expected positions $n\omega_c/\gamma$, since the frequency axis ticking is performed approximately, based only on the initial energy of the electron, and thus not taking into account the energy variation along the orbit.

In the spectrum of Fig. 7(c), the major difference with the typical cyclotron form is that the power corresponding to each harmonic does not follow the scaling β^n. This is due to the additional force of the external wave acting on the plasma, which is altering the rotation of the electrons with respect to the one induced solely by the magnetic field. A visualization of this comes with the comparison of cases (b) and (c), relevant to a small and large value of A_0 for a weakly-relativistic electron. In case (d) the electron is relativistic, the lines are very dense and the spectrum becomes similar to the form indicative of synchrotron radiation, with any differences owed again to the external wave.

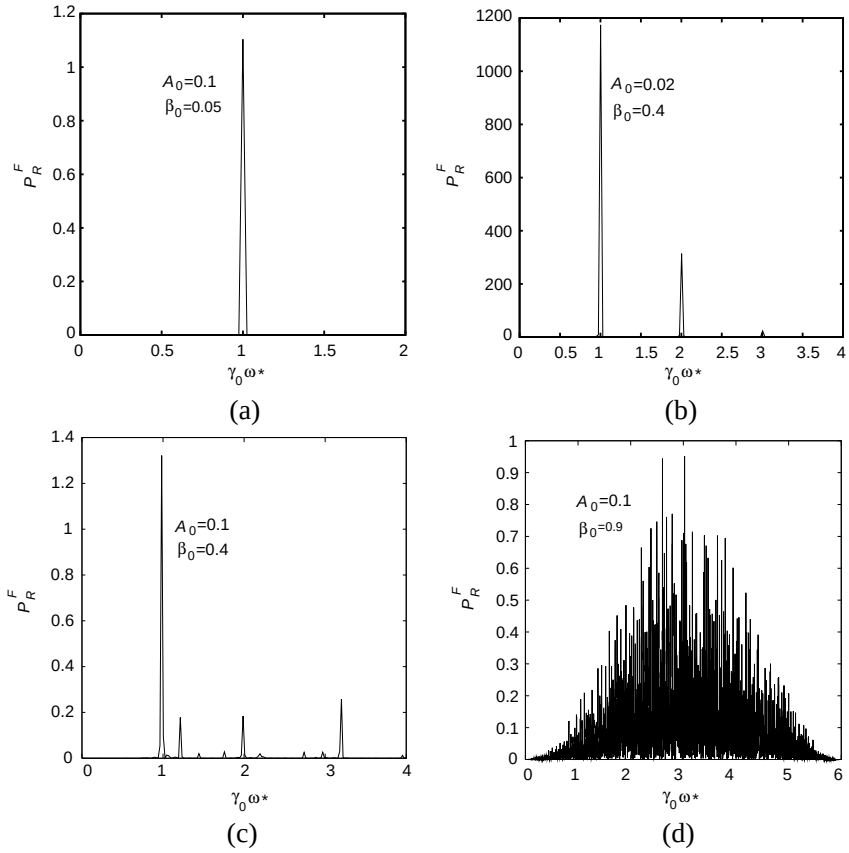

Figure 7. Power spectrum of the cyclotron radiation from a wave-driven magnetized electron for four different cases of the wave amplitude and the initial electron velocity.

5. CONCLUSION

Radio-frequency electromagnetic waves are the major force behind electron acceleration in the interplanetary plasma, whereas they are also used for plasma heating and current drive in thermonuclear fusion. In their turn, accelerated electrons emit radiation which provides a diagnostic for the plasma dynamics and generates an additional braking force known as radiation reaction. The improvement of the modeling of electron-cyclotron radiation, beyond the current state-of-the-art which is based on the assumptions of black-body emission and complete self-absorption by the plasma electrons, is crucial for the

accurate estimation of the synchrotron losses in applications.

In this paper, the cyclotron radiation by magnetized relativistic electrons driven by a plane radio-frequency wave has been studied in time and frequency domain. The particle orbits are calculated by solving the canonical equations of motion and the radiation in time and frequency domain is computed based on this data. In time-domain, the analysis has been done on the total power of emitted radiation, whereas in the frequency domain the radiation spectrum for electrons in all velocity ranges has been calculated from the microscopic orbits, using a novel algorithm on the basis of fast Fourier integral computation method. Since, in this problem, the orbits are chaotic after a threshold value for the external wave amplitude (acting as a dynamic perturbation), the computation has been performed for many values of the wave amplitude near and beyond that threshold.

The main results are the following: the instantaneous power is proportional to the acceleration, therefore it depends on the statistical properties of the Lorentz force. The electrons emit important quantities of radiation only for amplitudes over the threshold to chaos. The spectrum resembles to the one of cyclotron radiation: for lower energy only few harmonics appear, whereas for relativistic energies the spectrum takes the synchrotron form. The spectrum is computed very fast in terms of a novel algorithm, based on the fast Fourier transform, instead of the usual summation on the particle orbits. It is advisable that the form of the spectrum might be importantly modified depending on the modification of the energy along the electron orbit.

In order to reckon properly the results of this paper for the treatment of problems in fusion plasmas, like, e.g., the assessment of current drive efficiency in high-temperature plasmas (see, e.g., [22]), some limitations in the currently available model must be overcome. Primarily, a realistic toroidal magnetic geometry must be introduced [23]. This has as a consequence the complication of the mathematical expression for the vector potential amplitude of the wave, beyond the expression given in Eq. (2), and the need for reformulation of the Hamiltonian model. An alternative treatment may be based on Newton's equation of motion, which is considered in our current work.

Other important upgrades for our model should be the use of Maxwellian distribution for the electron initial energy, the inclusion of bremsstrahlung losses and the self-consistent computation of the electron motion, taking into account the deceleration due to the energy losses by radiation. In the equations of motion, the effect of the radiation should be reflected to a higher-order radiation reaction term (Abraham-Lorentz-Dirac force). For weakly-relativistic electrons the

relevant task is straightforward, however at larger energies a mass renormalization technique is required (details may be found in [6]).

ACKNOWLEDGMENT

The author would like to thank Prof. L. Vlahos, Dr. K. Arzner and Dr. H. Isliker for the very helpful discussions. This work has been sponsored by the European Fusion Programme (Association EURATOM-Hellenic Republic) and the Hellenic General Secretariat of Research and Technology. The sponsors do not bear any responsibility for the content of this work.

REFERENCES

1. Rybicki, G. B. and A. P. Lightman, *Radiative Processes in Astrophysics*, J. Wiley and Sons, New York, 1979.
2. Jackson, J. D., *Classical Electrodynamics*, Wiley, Boston, 1999.
3. Sitenko, A. G. and K. N. Stepanov, "On the oscillations of an electron plasma in a magnetic field," *Soviet Phys. JETP*, Vol. 4, 512, 1958.
4. Trubnikov, B. A., "On the angular distribution of cyclotron radiation from a hot plasma," *Phys. Fluids*, Vol. 4, 195, 1961.
5. Ternov, I. M., "Synchrotron radiation: A review," *Phys. Uspekhi*, Vol. 38, 409, 1995.
6. Barut, A. O., *Electrodynamics and Classical Theory of Fields and Particle*, Courier Dover Publications, London, 1980.
7. Farrell, W. M., M. D. Desch, and P. Zarka, "On the possibility of coherent cyclotron emission from extrasolar planets," *J. Geophys. Res.*, Vol. 104, 14025, 1999.
8. Feldman, U., E. Landi, and N. Schwadron, "On the sources of fast and slow solar wind," *J. Geophys. Res.*, Vol. 110, Art. A07109, 2005.
9. Leyser, T. B., B. Thide, H. Derblom, A. Hedberg, B. Lundborg, B. Stubbe, H. Kopka, and M. T. Rietfeld, "Stimulated electromagnetic emission near electron cyclotron harmonics in the ionosphere," *Phys. Rev. Lett.*, Vol. 63, 1145, 1989.
10. Rao, N. N. and D. J. Kaup, "Excitation of electron cyclotron harmonic waves in ionospheric modification experiments," *J. Geophys. Res.*, Vol. 97, 6323, 1992.
11. Courant, E. D. and M. S. Livingston, "The synchrotron: A new high energy accelerator," *J. Phys. Rev.*, Vol. 88, 1190, 1952.

12. Albajar, F., M. Bornatici, F. Engelmann, and A. B. Kukushkin, "Benchmarking of codes for calculating local net EC power losses in fusion plasmas," *Fusion Sci. Tech.*, Vol. 55, 76, 2009.
13. Polevoi, A. R., S. Y. Medvedev, T. Casper, Y. V. Gribov, A. A. Ivanov, J. A. Snipes, D. J. Campbell, and V. A. Chuyanov, "Assessment of operational space for longpulse scenarios in ITER," *Proc. 37th EPS Conference on Controlled Fusion and Plasma Physics*, Post. 2.187, 2010.
14. Ginzburg, V. L. and S. I. Syrovatskii, "Developments in the theory of synchrotron radiation and its reabsorption," *Ann. Rev. Astron. Astrophys.*, Vol. 7, 375, 1969.
15. Menyuk, C. R., A. T. Drobot, K. Papadopoulos, and H. Karimabadi, "Stochastic electron acceleration in obliquely propagating EM waves," *Phys. Rev. Lett.*, Vol. 58, 2071, 1988.
16. Karimabadi, H. and V. Angelopoulos, "Arnold diffusion in two dimensions," *Phys. Rev. Lett.*, Vol. 62, 2342, 1989.
17. Hizanidis, K., L. Vlahos, and C. Polymilis, "Diffusive electron acceleration by an obliquely propagating electromagnetic wave," *Phys. Fluids B1*, Vol. 3, 675, 1989.
18. Stix, T. H., *Waves in Plasmas*, Springer-Verlag, New York, 1992.
19. Tsironis, C. and Vlahos, L., "Anomalous transport of magnetized electrons interacting with electron-cyclotron waves," *Plasma Phys. Control. Fusion*, Vol. 47, 131, 2005.
20. Goldstein, H., *Classical Mechanics*, Addison-Wesley, Berlin, 1980.
21. Press, W. H., S. A. Teukolsky, W. T. Vellerling, and D. P. Flannery, *Numerical Recipes in Fortran*, Cambridge University Press, Cambridge, 1993.
22. Poli, E., E. Fable, G. Tardini, H. Zohm, D. Farina, L. Figini, N. B. Marushchenko, and L. Porte, "Assessment of ECCD-assisted operation in DEMO," *Proc. EC-17*, Art. 01005, 2012.
23. Tsironis, C., "On the simplification of the modeling of electron-cyclotron wave propagation in thermonuclear fusion plasmas," *Progress In Electromagnetics Research B*, Vol. 47, 37–61, 2013.